Title

SYSTEMATICS OF COMPLEX FRAGMENT EMISSION FROM LA INDUCED REACTIONS AT E/A = 47 MEV

Authors

Kehoe, W.L.
Mignerey, A.C.
Bradley, S.

Publication Date

1989-03-01

Lawrence Berkeley Laboratory
UNIVERSITY OF CALIFORNIA

Presented at the XXVII International Winter Meeting on
Nuclear Physics, Bormio, Italy, January 23–27, 1989

Systematics of Complex Fragment Emission from La Induced Reactions at E/A = 47 MeV

W.L. Kehoe, A.C. Mignerey, S. Bradley,
A. Marchetti, D.R. Bowman, R.J. Charity,
N. Colonna, H. Han, K. Jing, R.J. McDonald,
M.A. McMahan, L. Vinet, G.J. Wozniak,
L.G. Moretto, A. Moroni, and I. Iori

March 1989

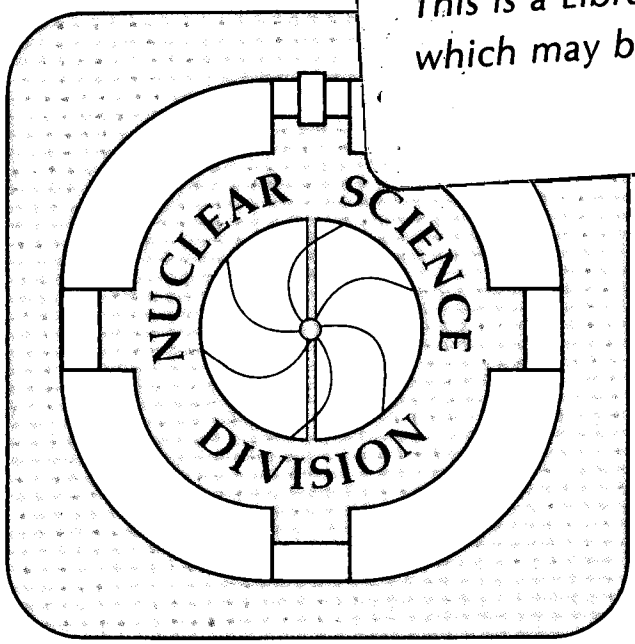

Prepared for the U.S. Department of Energy under Contract Number DE-AC03-76SF00098.

DISCLAIMER

SYSTEMATICS OF COMPLEX FRAGMENT EMISSION FROM La INDUCED REACTIONS AT E/A = 47 MeV*

W.L. Kehoe, A.C. Mignerey, S. Bradley§, and A. Marchetti
Department of Chemistry, University of Maryland, College Park, Maryland 20742, U.S.A.

D.R. Bowman, R.J. Charity◊, N. Colonna, H. Han#, K. Jing#, R.J. McDonald, M.A. McMahan, L. Vinet‡, G.J. Wozniak, and L.G. Moretto
Nuclear Science Division, Lawrence Berkeley Laboratory, 1 Cyclotron Road, Berkeley, California 97420, U.S.A.

A. Moroni and I. Iori
Department of Physics, University of Milano and Istituto Nazionale di Fisica Nucleare, Sezione di Milano,Via Celoria 16, 20133, Milano, ITALY

Abstract: Complex fragment (Z > 2) emission was studied in the reverse kinematics reactions of ^{139}La on ^{27}Al and $^{nat.}$Cu at a bombarding energy of E/A = 47 MeV. Experimental results from inclusive and coincidence measurements for two- and three-fold complex fragments events are presented. Measured cross sections and Z_1 - Z_2 correlations show a predominatly binary-decay process for the La + Al reaction, while the La + Cu reaction is dominated by multi-body decay.

1. Introduction

At low bombarding energies (E/A ≤ 10 MeV) Sobotka *et al.* have shown complex fragments (2 < Z < 1/2 Z_{CN}) are emitted with very low cross sections from compound nuclei produced by the complete fusion of the target-projectile system.[1] At still higher energies (E/A ≤ 50 MeV/u) complex fragments have been shown to be produced from the binary statisical emission of a compound nucleus formed during either complete or incomplete fusion processes.[2-4] These results are in agreement with a theory by Moretto that predicts complex fragment production as a compound nucleus binary decay mode ranging between the extremes of light particle evaporation and fission.[5]

Other studies in this energy range have shown the importance of non-equilibrium processes for light complex fragment production. Up to 50% of the cross section of light complex fragments $Z \leq 12$ could be accounted for by non-equilibrium emission in the reaction N + Ag at E/A = 20 - 50 MeV.[6] A number of multifragmentation models have been proposed, based on either statistical or dynamical mechanisms, to explain fragment production in the intermediate energy regime (E/A = 10 - 100 MeV). The models of Bondorf[7], Zhang and Gross[8,9], and Cerruti and Ngo[10,11] predict the onset of multifragmentation in the excitation energy range of 4 - 5 MeV/u. At higher bombarding energies, like central Au + Au collisions at E/A = 200 MeV, large (8 - 9) average complex fragment multiplicity events have been interpreted as evidence of a multifragmentation process.[12]

A previous study by our collaboration showed that complex fragments produced in the reaction La + C at E/A = 50 MeV came from the binary-decay of a compound nucleus-like source, formed via the incomplete fusion of the La with approximately half the mass of the C target.[13] The extracted momentum transfer of 53% and excitation energy of 1.9 MeV/u were consistent with momentum transfer systematics.[14] Using his model Gross reproduced the fragment-fragment correlations measured in this reaction, concluding that there was a clear multifragment nature to the reaction.[15] Motivated by the continued presence of a compound nucleus-like source which produces complex fragments via statistical emission, and by predictions for the onset of multifragmentation at higher excitation energies, we have chosen to extend this work by studying the systems La + Al and Cu at E/A = 47 MeV. Momentum transfer systematics predict that by increasing the target mass of the reacting system the available excitation energy should reach the limit for the onset of multifragmentation.

2. Experimental Method

Beams of approximately 10^7 particles per pulse of 47 MeV/u ^{139}La were provided by the BEVALAC accelerator complex of the Lawrence Berkeley Laboratory. The ^{139}La projectiles were incident on targets of ^{27}Al (3.3 mg/cm^2) and ^{nat}Cu (1.9 mg/cm^2).

The reaction products with $Z > 2$ were detected with ten position-sensitive ΔE - E telescopes, configured in an array about the beam as shown in fig. 1. Each telescope consisted of three detectors: a 300 μm Si, a 5 mm Si(Li), and a 7.6 cm BC400 plastic. These telescopes were designed for measuring the atomic charge, energy and position of fragment events from reverse kinematics reactions.[16] The array was placed 40 cm from the target, and mounted so that the center of each telescope was normal to the target. The front face of each telescope was 55 mm x 57 mm, with an active-area of 44.8 mm x 44.8 mm (64%). The active-area angular-acceptence of each detector was 6.4°, while the packaged telescope coverage was 8.2°. The in-

plane telescope was ±3.4° to ±18° and the out-of-plane coverage was to ±12.7°, each realative to the beam direction.

The energy calibrations were obtained by exposing the silicon detectors to low intensity (~10^3 particles per pulse) La beams at 27 and 47 MeV/u. The lower energy beam was produced by degrading the 47 MeV/u beam with an Al degrader. Electronic pulsers were used to check the consistency of the calibration values. Corrections were made for the pulse-height defect using the systematics of Moulton *et al.*[17], and for the energy loss through a thin Au foil in front of the 300 μm Si, used for suppressing electrons and X-rays.

The large dynamic range of the silicon ΔE - E telescopes allowed for the identification of all charged particles up to the projectile (Z = 57). Only results from these two element telescopes are discussed below. Figure 2 shows the charge distribution measured in the A5 telescope from the La + Al reaction. The peaks associated with charged particles up to Z = 51 are clearly observed. Punch-through of light charged particles through the 5 mm Si(Li) detector was responsible for the decreased yield of products with Z ≤ 5.

The silicon detectors were position sensitive in one dimension. This was acheived by charge division using 15 implanted boron strips in the 300 μm Si detectors and 15 Au-Pd strips evaporated on the 5 mm Si(Li) detectors. The 300 μm Si and 5 mm Si(Li) detectors were rotated 90° relative to each other to determine both the x- and y-positions of charged particles traversing the telescope. An example of the position resolution obtained from the 5 mm Si(Li) detectors is shown in fig. 3 for the A5 telescope. The 15 strips are clearly resolved, with each strip corresponding to about 0.4°.

The absolute cross sections were normalized with respect to beam charge collected in a Faraday cup. All inclusive and coincident events were recorded event-by-event on magnetic tape and analyzed off-line.

3. Results

3.1 Velocity Diagrams

Linear density plots of the inclusive cross section ($\partial^2\sigma/\partial V_{par}\partial V_{per}$) in the V_{par} - V_{per} plane for representative detected atomic charges are shown in figs. 4 and 5 for the La + Al and Cu reactions at E/A = 47 MeV/u. The velocity corresponding to complete fusion of the target-projectile system is shown by the solid arrow, while the beam velocity is shown by the dashed arrow. The velocity of the complex fragment was determined from its measured energy and atomic charge (Z). The atomic mass (A) of the fragment was calculated from the measured Z-value using the parameterization

$$A = 2.08Z + 0.0029Z^2, \quad (1)$$

which was shown to be adequate for the systems studied[2]. For the La + Al reaction in fig. 4, a trend is observed from backward (Z = 6 - 14) to sideways (Z = 18) to forward (Z = 22 - 38) peaking of the yield for the emitted complex fragments. This trend evolves sooner for the La + Cu reaction, fig. 5; where the yield is forward peaked already by Z = 18

Particle emission from a compound nucleus binary-decay is characterized by a Coulomb circle in the velocity plane, since the emission velocity of the particle is determined mostly by the Coulomb repulsion between it and its partner. This has been shown by Charity *et al.* for similar system at lower bombarding energies[2] and in the 50 MeV/u La + C reaction[13]. However, the velocities of complex fragments in the V_{par} - V_{per} plane for the La + Al and Cu reactions at E/A = 47 MeV do not generate circles, but ellipses. Depending upon the impact parameter and transferred momentum, binary or sequential-binary decay can have ellipitically shaped emission velocities in the V_{par} -V_{per} plane if compound nuclei are formed in incomplete fusion reactions with a range of source velocities[18].

3.2 Z_1 - Z_2 Correlations

The inclusive cross section plots for the La + Al and Cu reactions do not show explicity the multiplicity (n = 2,3,4,...). The multiplicity can be seen implicity in plots of the Z_1 - Z_2 correlations in coincidence events, where Z_1 and Z_2 are the atomic charges of the detected particles in any two of the ten telescopes. Figures 6(a) and (b) show the Z_1 - Z_2 correlation plots, along with the assoicated sum charge ($Z_1 + Z_2$) spectra, for the two- (n = 2) and three-fold (n = 3) multiplicity events of Z > 3 in the La + Al reaction. Figures 7(a) and (b) show the same plots for the La + Cu reaction. In figs 6(b) and 7(b) Z_2 represents the sum charge of the second and third particles detected in three of the ten telescopes. Statistics were not adequate to make similar plots for the four-fold (n = 4) coincidence events. These plots show an enhancement along the Z_2 axis at low Z_1 values due to the asymmetry of the telescope positions around the beam.

In the two-fold Z_1 - Z_2 correlation plot for the La + Al reaction a broad band along a line of approximately constant value of $Z_1 + Z_2$ and a well defined peak in the sum charge spectrum at Z_{tot} = 49 shows evidence for a two-body decay process. This result is similar to that of the La + C system at E/A = 50 MeV, which was shown to be consistent with the decay of a compound nucleus-like system formed by an incomplete fusion reaction. The broad width of the sum charge distribution may be the result of a range of impact parameters and, therefore,

momentum transfers available to the reacting system. A smaller peak is obsevred in the sum charge distribution for the two-fold coincidence events at low Z_{tot} values due to detecting only two complex fragments from a $n \geq 3$ multiplicity events. The three-fold coincidence events for the La + Al reaction continue to show a band of approximately constant $Z_1 + Z_2$ in the correlation plots and a peak at $Z_{tot} = 48$ in the sum charge distribution. The peak at low Z_{tot} in the $n = 2$ sum charge distribution has now shifted to higher Z_{tot} values when a third fragment was detected, as shown in the sum charge distribution for the $n = 3$ coincidence events.

The characteristic band in the Z_1 - Z_2 plot disappears and is replaced by an even filling in of the Z_1 - Z_2 correlation plots for the La + Cu reaction. The sum charge distribution for the two-fold multiplicity covers a wide range of available charge with a mean value of $Z_{tot} \sim 25$, while the three-fold sum charge is less broad and gaussian shaped with a mean detected charge of $Z_{tot} \sim 34$. The narrowing of this distribution for the three-fold coincidence events indicates that most of the $n = 2$ events are associated with incomplete detection of the emitted complex fragments for the La + Cu reaction. This missing charge can be the result of: 1) large numbers of light particles ($Z \leq 2$) emitted during the preequilibrium stages of the reaction or evaporatd from the primary fragments, and/or 2) some complex fragments are emitted kinematically beyond the range of the array.

In comparing the La + Al and La + Cu sum charge distributions, the detected mean charge decreases as the target mass increases. This trend correlates with the expected increase of available center-of-mass energies from 4.2 MeV/u to 7.2 MeV/u for the Al and Cu targets, respectively, calculated from momentum transfer systematics.[14]

3.3 Source Velocities

Center-of-mass velocities for the events associated with the reactions under consideration were determined from the velocities of the detected fragments in either the two- or three-fold coincidence events. The extracted center-of-mass velocities spanning the range all Z-values are shown in fig. 8(a) for the La + Al reaction and fig. 8(b) for the La + Cu reaction, plotted as the ratio of the source velocity relative to the beam velocity (V_{source}/V_{beam}). As in figs. 4 and 5, the velocity corresponding to complete fusion of the target-projectile system is shown by the solid arrow, while the beam velocity is shown by the dashed arrow. These distributions were fit with a gaussian and the centroids of V_s/V_b for each reaction and multiplicity are presented in table 1. These values are still priliminary and the systematic uncertainties due to the energy calibrations and mass parameterization have not yet been evaluated. However, the qualitative trends should not change.

TABLE 1

Extracted source volocities relative to the beam velocity summed over all Z-values ≥ 3 for reactions with 47 MeV/u ^{139}La

Target	^{27}Al	^{27}Al	$^{nat.}$Cu	$^{nat.}$Cu
multiplicity	n=2	n = 3	n = 2	n = 3
V_{source}/V_{beam}	0.94	0.93	0.92	0.89

The shape of the V_s/V_b distributions and the mean values are very similar for the two- and three-fold coincidence events with the Al target. When considered with the sum charge distributions (insets in figs. 6 and 7) for these reactions, the nearly identical center-of-mass velocities are not surprising, since in each case the majority of the charge is detected. The shoulder in the distribution at $V_s/V_b \geq 0.90$ for the Al two-fold coincidence events corresponds to the peak at the low Z_{tot} in the sum charge distribution, assoicated with n > 2 events. The V_s/V_b distributions for the Cu target have similiar shapes and values for the two- and three-fold coincidence events. However, for the Cu target, the sum charge distributions for n = 2 and n = 3 are very different. As with the Al target, the V_s/V_b distribution also shows a shoulder at low values due to incomplete detection of the emitted fragments.

For both targets the available velocity range between V_{beam} and the velocity of complete fusion for the projectile-target system is filled by the observed events. With 47 MeV/u ^{139}La and these relatively light targets, the reverse kinematic technique compresses the range of allowed source velocities into a very narrow range. This might account for the observation that the centriods of the V_s/V_b distributions for this beam energy are independent of the target mass, yet allow for different shapes in the assoicated sum charge distributions.

3.4 Cross Sections

Angle-integrated cross sections were calculated from the yields of the emitted complex fragments by fitting 2nd-order polynomials to the angular distribution. The cross sections, as a function of the detected atomic charge, for the La + Al and Cu reactions are shown in fig. 9. The charge distribution for the La + Al system decreases monotonically until it flattens out between the range of 10 to 15 mb at Z > 15. This shape is in sharp contrast to the shape observed at lower energies which has a peak at symmetry, typical of systems above the Businaro-Gallone point.[2] At the highest Z-values the charge distribution shows a slight hint of

rising near symmetry. This is might be evidence that the complex fragment production was from the statistical decay of a very hot compound nucleus-like system. Unfortunately, the detector array was kinematically limited from measuring these Z-value fragments.

Evidence for the multi-body decay of the La + Cu reaction is shown in the shape of the monotonically decreasing cross section with increasing Z-value. The cross section for the Cu target in the range of $5 < Z < 30$ is about three-to-four times greater than that for the Al target. The multi-body decay of the Cu target is not surprising considering the large amount of excitation energy available to the system.

4. Conclusion

Complex fragments ($Z > 3$) were measured in the reactions of ^{139}La on ^{27}Al and $^{nat.}Cu$ at bombarding energies of E/A = 47 MeV. Coincidence measurements presented in the Z_1 -Z_2 correlations and sum charge distributions, and the measured cross section for the Al target show that the reaction is primarily a two-body decay process, along with possibly sequential binary-decay accounting for the observed three-fold multiplicity events. This result is comparable to that of the 50 MeV/u La + C results of Bowman, *et al.*.[13] In contrast, the La + Cu system is dominated by multi-body decay. This correlates with the dramatic increases in the available center-of-mass energy from 4.2 MeV/u to 7.2 MeV/u for the La + Al and La + Cu systems. This multi-body decay may result from either a multiple sequential binary-decay mechanism or a prompt multifragmentation mechanism, which is predicted to occur within this range of excitation energies. The large charge deficit in the Z_{tot} distribution and the high yield of fragments below Z = 30 in the measured cross section indicates that the Cu reaction is an excellent candidate to study the decay of very hot systems.

References

* This work was supported by the Director, Office of Energy Research, Division of Nuclear Physics of the Office of High Energy and Nuclear Physics of the US Department of Energy under contracts DE-AC03-76SF00098 and DE-FG05-87ER40321.

§ Present address: Kaman Sciences, Alexandria, Virgina, U.S.A..

◊ Present address: GSI, D-6100, Darmstadt, West Germany.

Premanent address: Institute of Atomic Energy, Bejing, China.

‡ Present address: CERN, Division EP, Ch-12211, Geneva 23, Switzerland

1. L.G. Sobotka, et al.,Phys. Rev. Lett. **51** (1983) 2187 and Phys. Rev. Lett. **53** (1984) 2004.
2. R.J. Charity, et al., Phys. Rev. Lett. **56** (1986) 1354; Nucl. Phys. **A476** (1988) 516 and Nucl. Phys. **A483** (1988) 371.
3. G. Auger, et al., Z. Phys. **A321** (1985) 243.
4. F. Auger, et al., Phys. Rev. **C35** (1987) 190.
5. L.G. Moretto, Nucl.Phys. **A247** (1975) 211.
6. D.E. Fields, et al., Indiana University Nuclear Chemistry Preprint, INC-40007-52 (1988).
7. J.P. Bondorf, Nucl. Phys. **A443** (1985) 321c and Proceedings of the Texas A&M Synposium on Hot Nuclie, College Station, Texas, Dec. 7-10, 1987, World Scientific, Singapore (1988), p.321.
8. X.Z. Zhang, et al., Nucl. Phys. A461 (1987) 641.
9. D.H.E. Gross, Nucl. Phys. **A488** (1988) 217c.
10. C. Cerruti, et al., Nucl. Phys. **A476** (1988) 74.
11. C. Ngo, Nucl. Phys. **A471** (1987) 381c and Proceedings of the Texas A&M Synposium on Hot Nuclie, College Station, Texas, Dec. 7-10, 1987, World Scientific, Singapore (1988), p.354.
12. B.V. Jacak, Nucl. Phys. **A488** (1988) 325c.
13. D.R. Bowman, et al., Phys. Lett **189B** (1987) 282.
14. V.E. Viola, Nucl. Phys.**A471**, (1987) 53c.
15. D.H.E. Gross, Phys. Lett. **203B** (1988) 26.
16. W.L Kehoe, et al., Nuclear Science Division Annual Report 1985-1986, Lawrence Berkeley Laboratory publication LBL-22820 (1987), p.104.and p.106.
17. J.B Moulton, et al.,Nucl. Instr. Meth. **157** (1978) 325.
18. N. Colonna, et al., Lawrence Berkeley Laboratory preprint LBL-26459 (1988) and submitted to Phys. Rev. Lett..

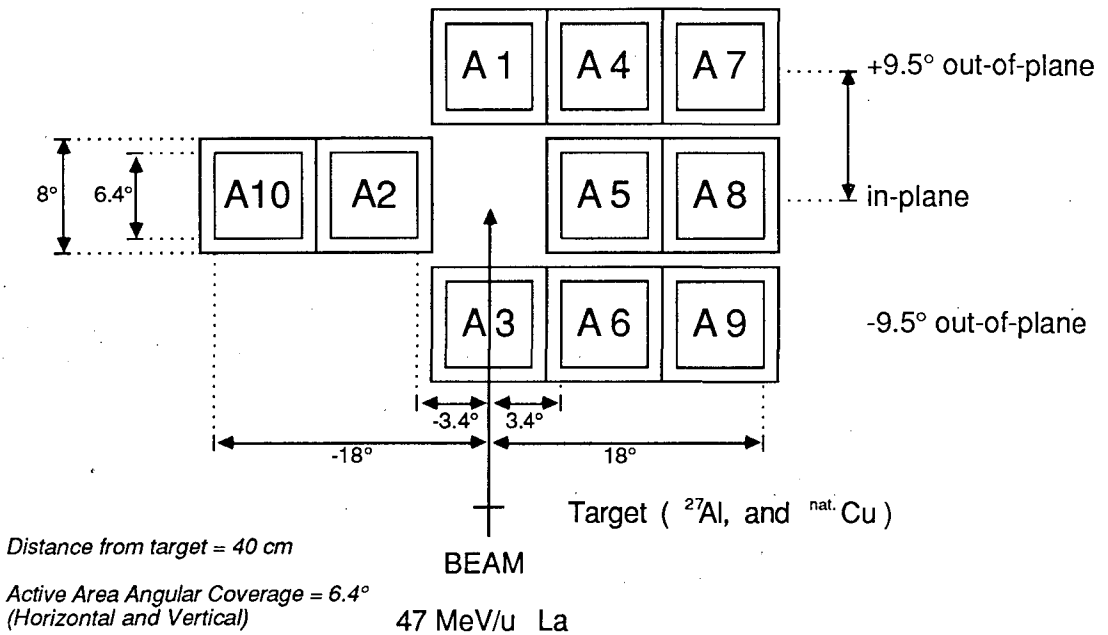

Fig. 1. Schematic diagram of the experimental setup of the ten three-element telescopes positioned around the beam.

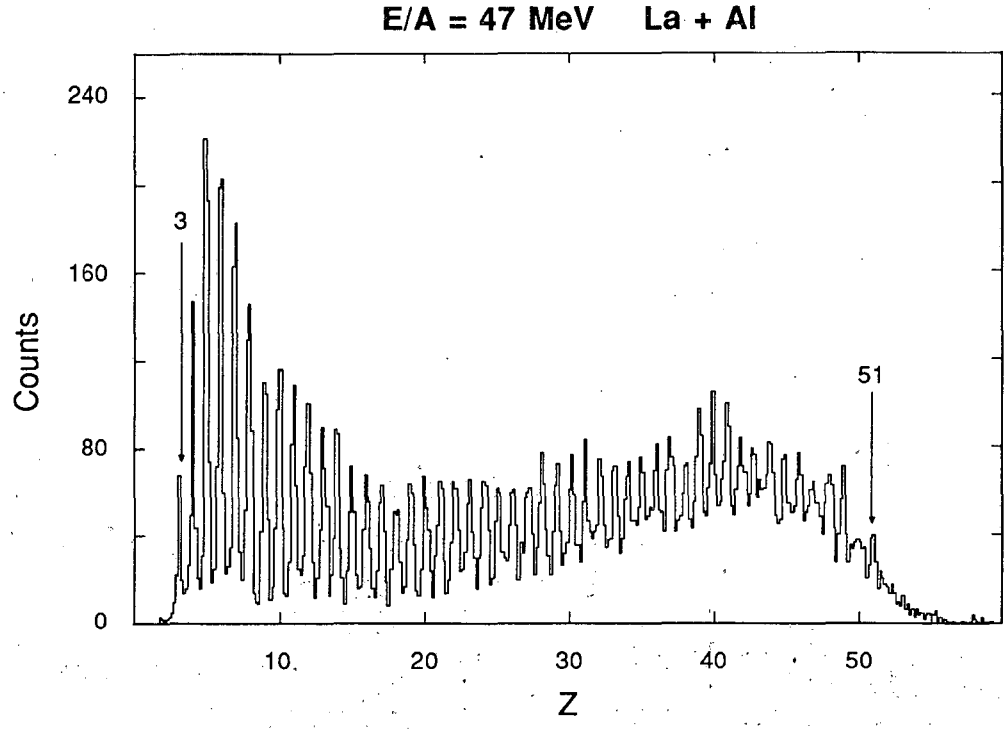

Fig. 2. Histogram of the Z resolution obtained uisng the 300 μm Si - 5 mm Si(Li) telescope for the La + Al reaction, showing charge particle identification from Z = 3 to Z = 51. The edgeof telescope A5 was 3.4° from the beam.

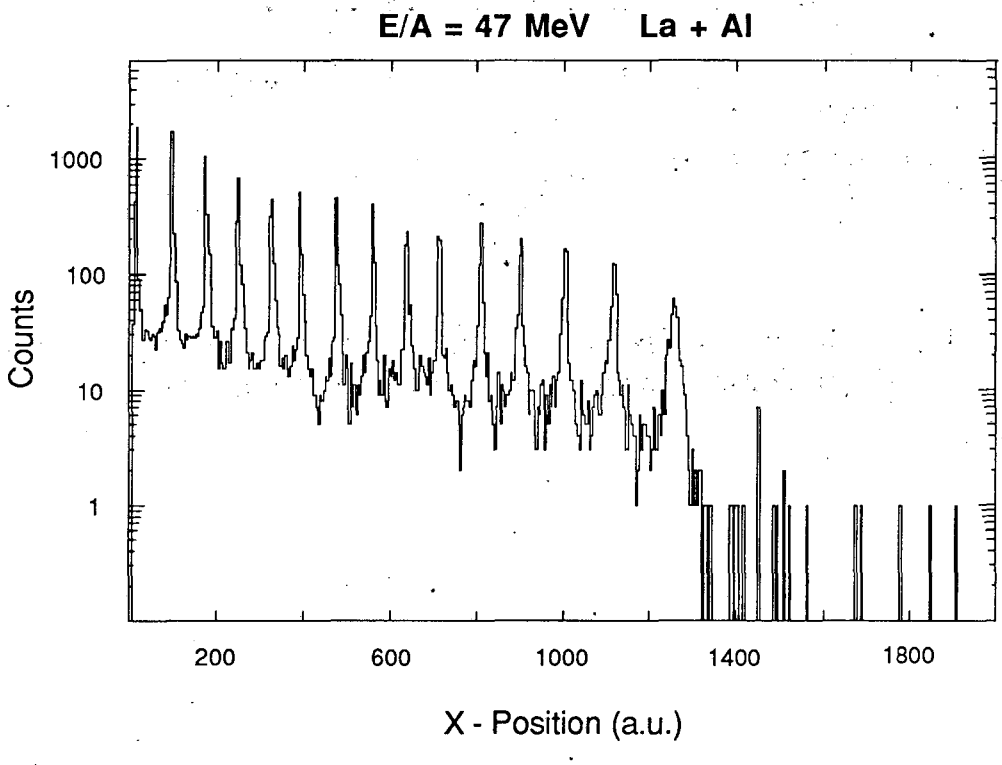

Fig. 3. Example of the position resolution from the 15 resistive chain strips on front of the 5 mm Si(Li) detector of the A5 telescope for the La + Al reaction.

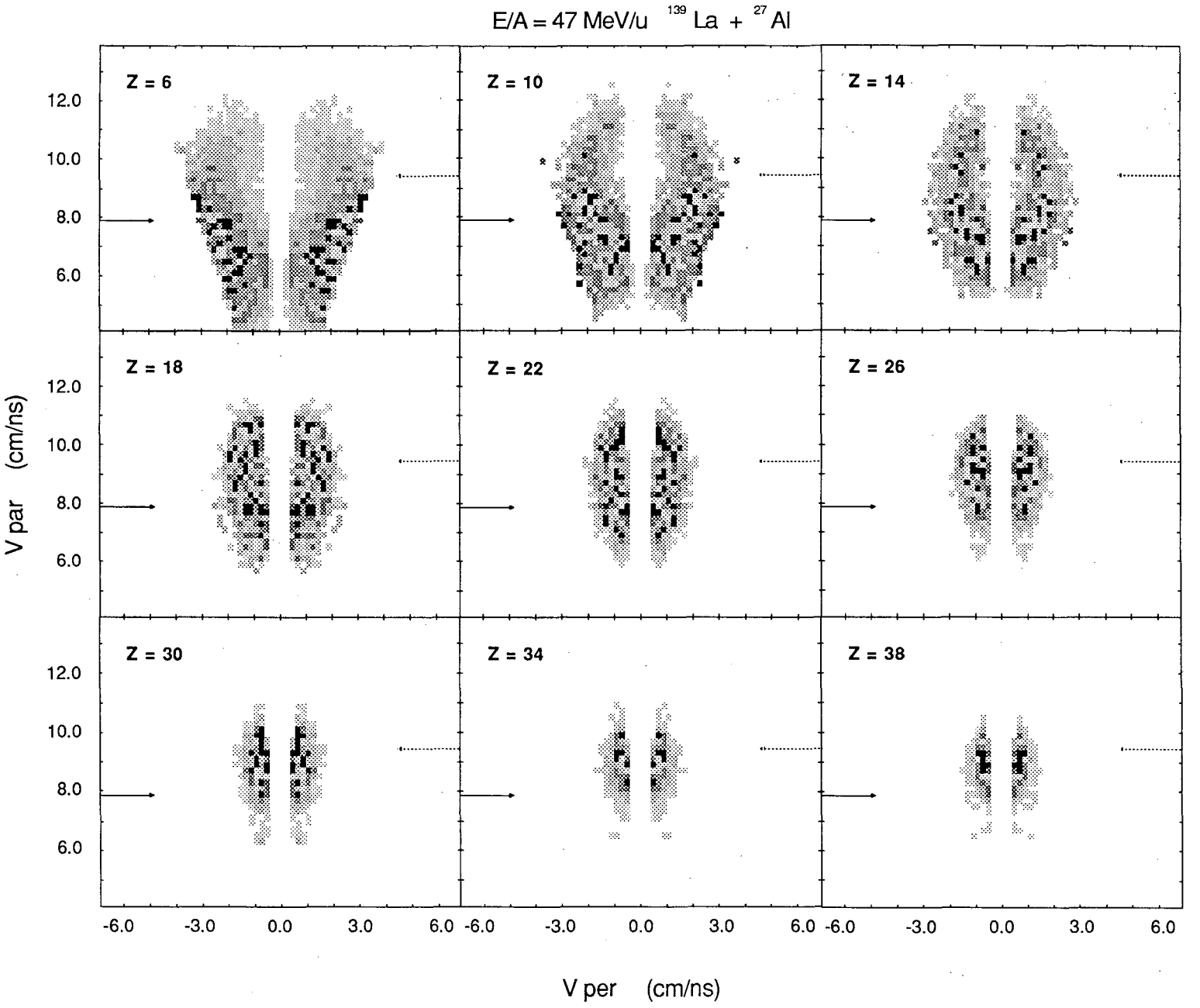

Fig. 4. Experiment inclusive cross section (∂sigma/∂Vpar-∂Vper) in the Vpar - Vper plane for representative fragment Z-values detected in the reaction E/A = 47 MeV La + Al. The velocity corresponding to complete fusion of the target-projectile system is shown by the solid arrow, while the beam velocity is shown by the dashed arrow.

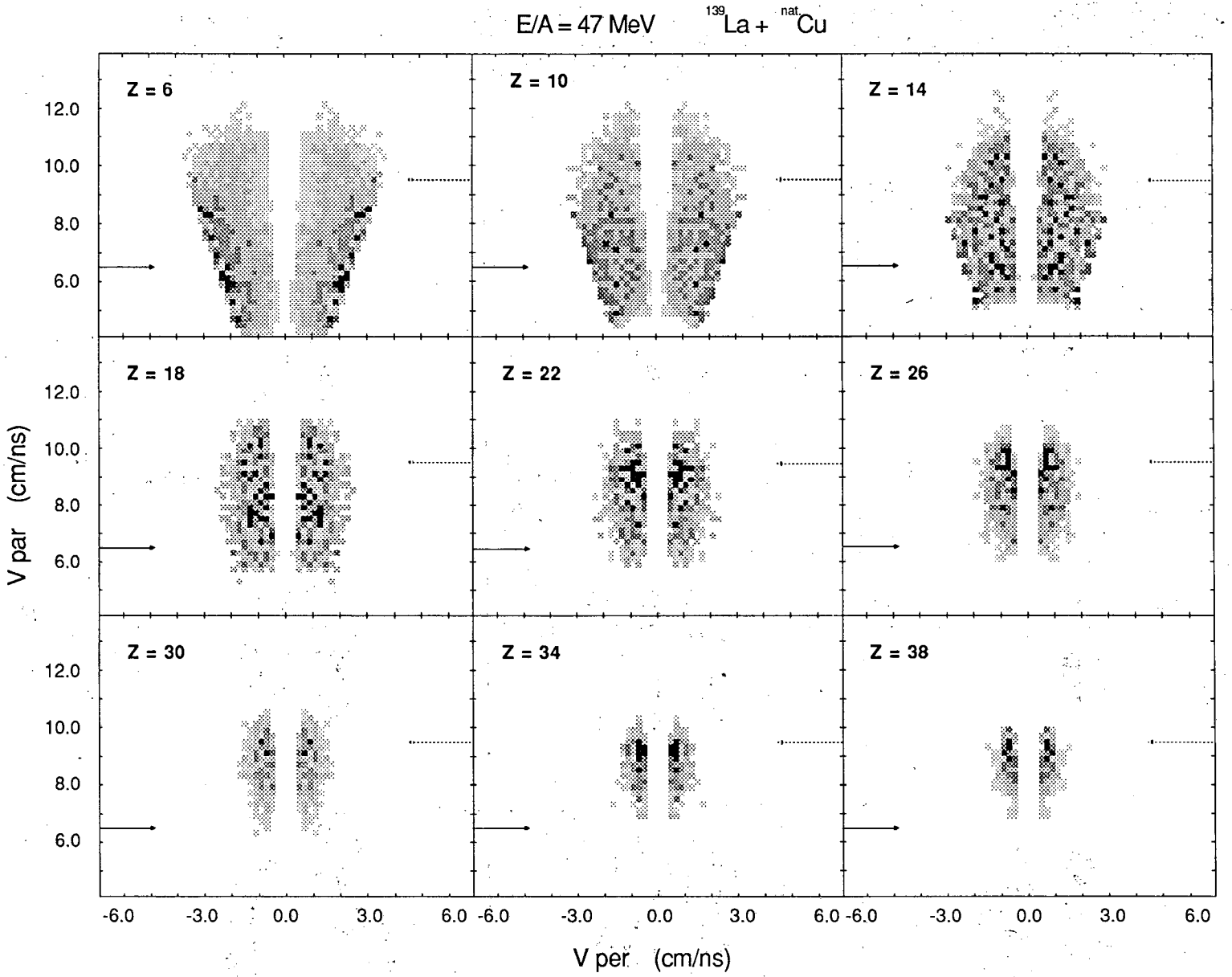

Fig. 5. Experiment inclusive cross section (∂sigma/∂Vpar-∂Vper) in the Vpar - Vper plane for representative fragment Z-values detected in the reaction E/A = 47 MeV La + Cu. The velocity corresponding to complete fusion of the target-projectile system is shown by the solid arrow, while the beam velocity is shown by the dashed arrow.

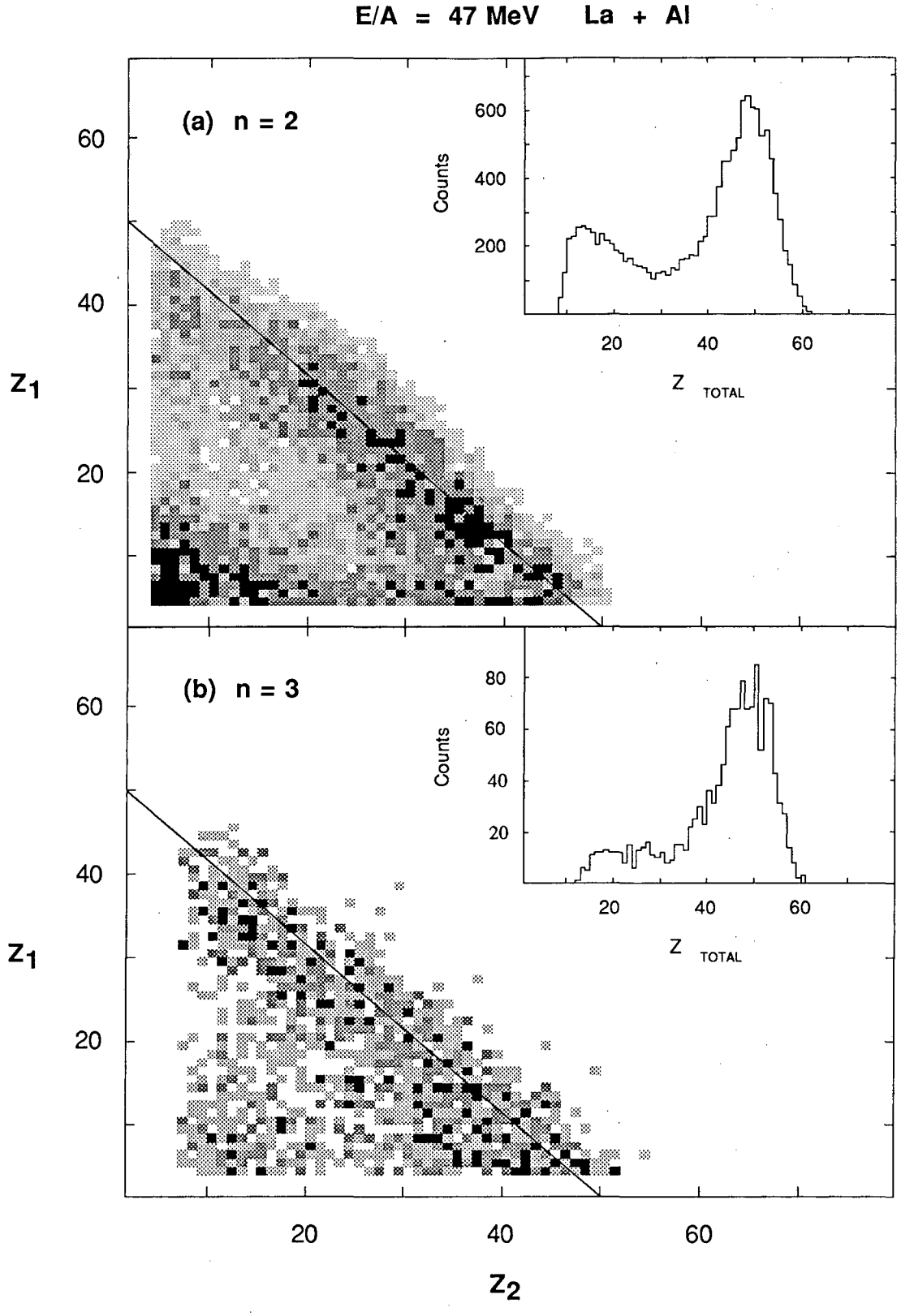

Fig. 6. (a) Fragment-fragment correlation plot for two-fold coincidence events with fragments $Z > 3$. (b) Same correlation plot for three-fold coincidence events, where $Z_2 = Z_2 + Z_3$. The inset spectra show the sum charge distribution $(Z_1 + Z_2)$ for the correlation plots. The solid line is to guide the eyes and corresponds to $Z_1 + Z_2 = 50$.

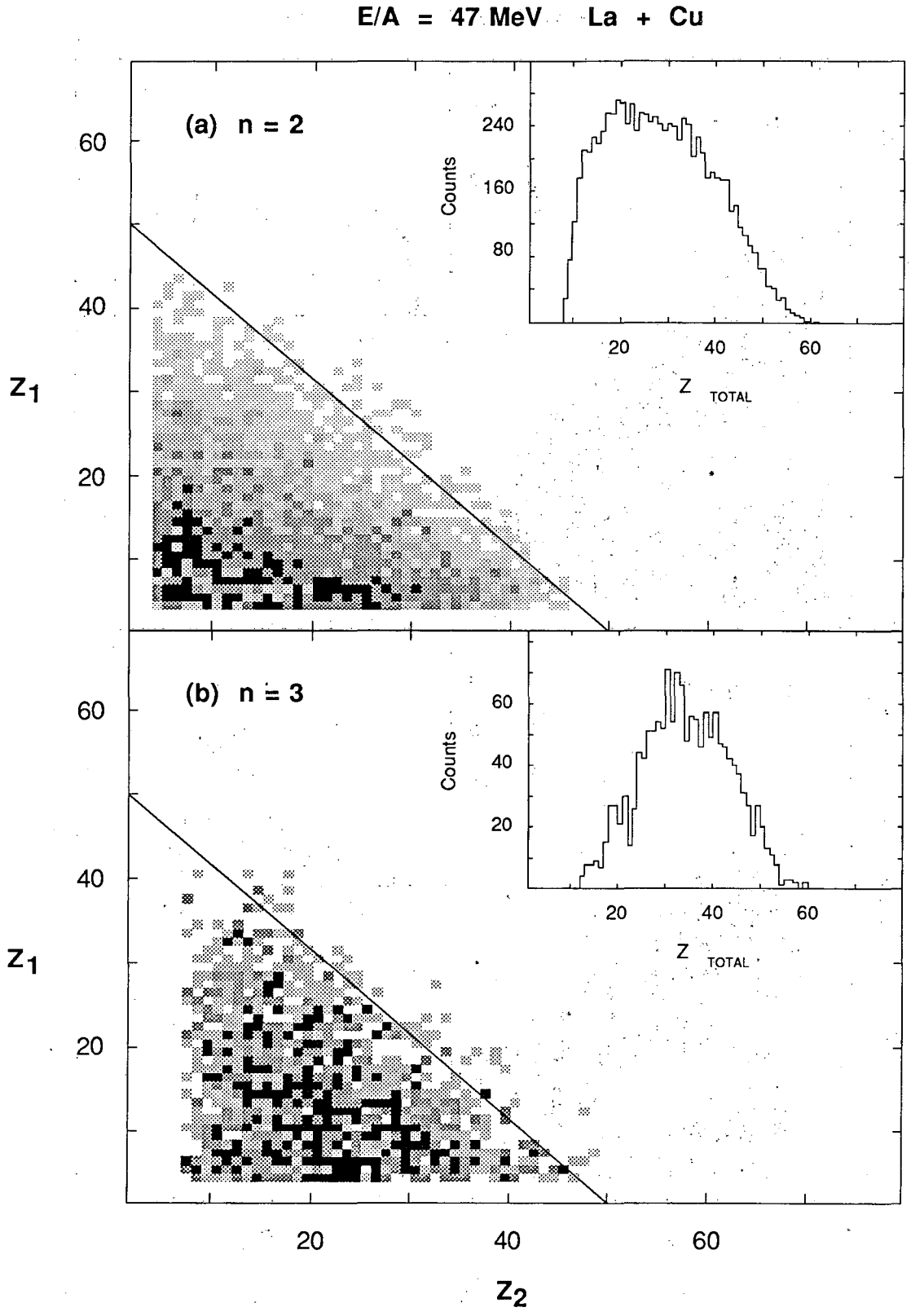

Fig. 7. (a) Fragment-fragment correlation plot for two-fold coincidence events with fragments $Z > 3$. (b) Same correlation plot for three-fold coincidence events, where $Z_2 = Z_2 + Z_3$. The inset spectra show the sum charge distribution $(Z_1 + Z_2)$ for the correlation plots. The solid line is to guide the eyes and corresponds to $Z_1 + Z_2 = 50$.

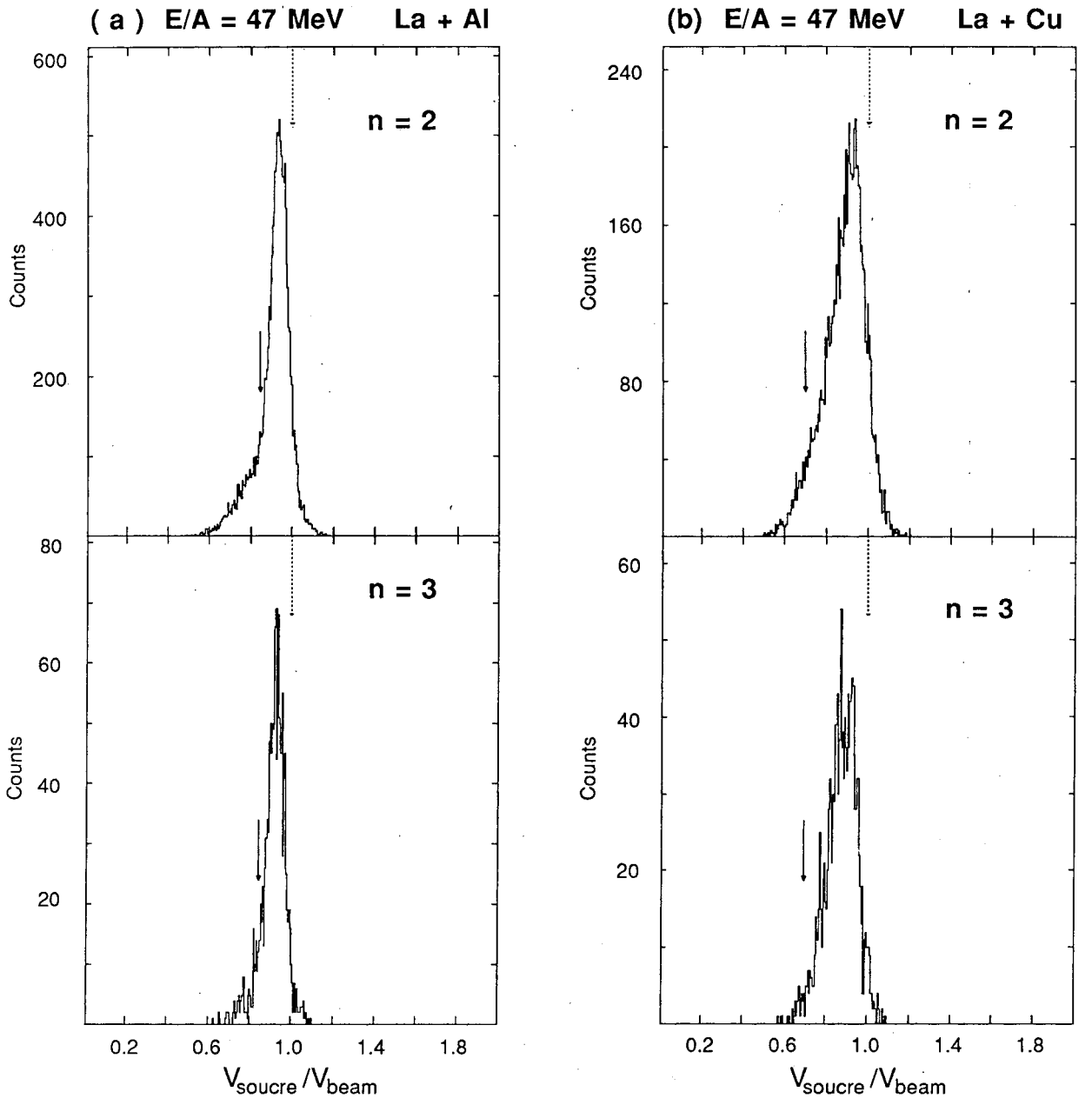

Fig. 8(a). Extracted center-of-mass velocities relative to the beam veolicty spanning the range of Z-values for the 47 MeV/u La + Al reaction for the two- and three-fold coincidence events. (b). The same figure for the 47 MeV/u La + Cu reaction. The velocity corresponding tocomplete fusion of the target-projectile system is shown by the solid arrow, while the beam velocity is shown by the dashed arrow.

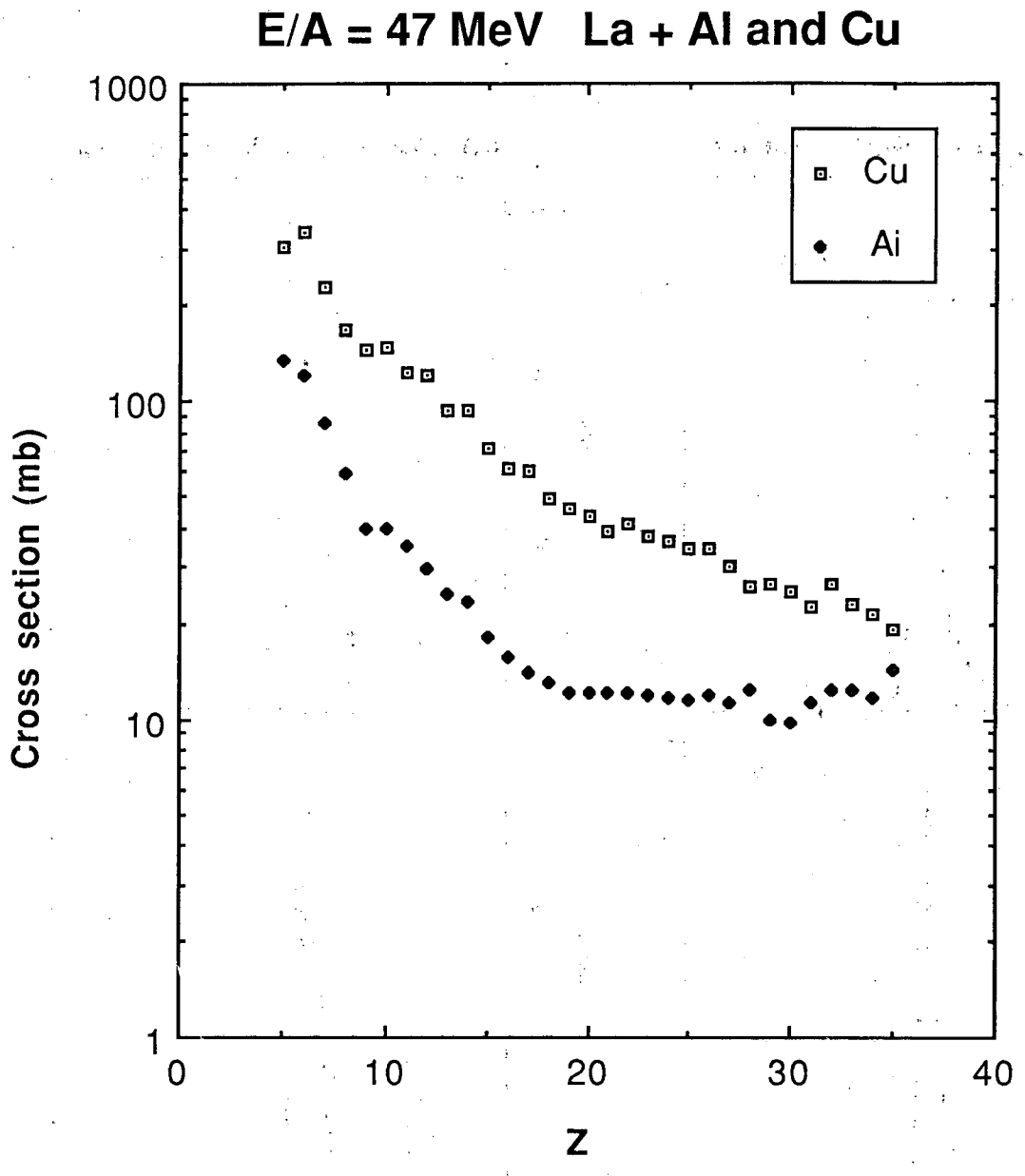

Fig. 9. Angle-integrated charge distributions of complex fragments produced in the reactions 47 MeV/u La + Al and Cu.

LAWRENCE BERKELEY LABORATORY
TECHNICAL INFORMATION DEPARTMENT
1 CYCLOTRON ROAD
BERKELEY, CALIFORNIA 94720